DOI: 10.1002/ange.201005431

Heavy-Atom Effect

^{29}Si DFT/NMR Observation of Spin–Orbit Effect in Metallasilatrane Sheds Some Light on the Strength of the Metal→Silicon Interaction**

Lionel A. Truflandier, Erica Brendler, Jörg Wagler, and Jochen Autschbach**

Relativistic effects in structural chemistry have long fascinated chemists.[1] Moreover, special relativity can induce spectacularly large effects on NMR parameters.[2] A well-known example is the normal halogen dependence (NHD) of isotropic shifts, which is a spin–orbit (SO) relativistic effect (a "heavy-atom effect" on a light atom, or HALA). Experimental clues for relativistic effects on chemical shift *tensors* are not as commonly looked for. Forgeron et al. demonstrated that relativistic effects play an important role in xenon NMR spectroscopy.[3] In this case, the heavy-atom effect is on the heavy-atom NMR itself (HAHA): For XeF_2, a 1000 ppm Xe chemical shift tensor component parallel to the molecular axis was found experimentally. In the absence of relativistic effects, this component is zero by symmetry. More recently, Kantola et al. showed that the well-known NHD in methyl halides also has a strong impact on the ^{13}C shielding anisotropies.[4] In addition to these particular examples, considering strong relativistic effects on NMR properties may in general turn out to be essential in the characterization of various classes of compounds, as shown in the literature, for example, for complexes with Pt- and Au-bound O atoms,[5] mercury organic compounds,[6] haloboranes,[7] and various phosphine complexes of main group and transition metals (TM).[8] Furthermore, fundamental insights into unusual bonding situations in novel compounds may be achieved only with the aid of models that take spin–orbit interactions into account.

As to the latter, one such novel bonding situation is represented by the formal σ-donation from an electron-rich TM (d^8 systems: Pd^{II}, Pt^{II}; d^{10} system: Au^{I}) as a Lewis base towards a Lewis acidic Group 14 element center (Si^{IV}). Recently, Bourissou and co-workers reported on an aurasilatrane with a rather long Au···Si separation (3.090(2) Å) and a somewhat upfield-shifted ^{29}Si resonance ($\delta^{29}Si = -21.4$ ppm for the formally pentacoordinate Si atom in an Si(F,C-(aryl)$_3$,Au) environment).[9] In contrast (from the ^{29}Si NMR perspective), two of us presented the paddlewheel-shaped compounds **1** and **2** comprising d^8-donor sites in closer proximity to the Si atom (Figure 1) and ^{29}Si resonances in the typical range of hexacoordinate Si atoms, which proved the metal atoms to be efficient lone-pair donors.[10]

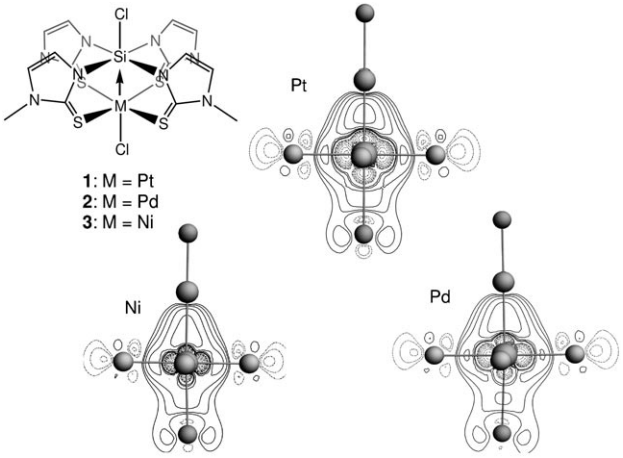

Figure 1. Structures of complexes **1**–**3**. Contour plots of the electron deformation densities with respect to promolecular $Cl[Si(\mu\text{-mt})_4]^-$, Cl^-, and M^{2+} fragments (mt = 2-mercapto-1-methylimidazolide). Full (dashed) lines indicate positive (negative) density values with contours between 5×10^{-3} and 2 au.

Following the initial report[10] of a significantly upfield (shielded) ^{29}Si isotropic chemical shift for Pt compound **1** ($\delta = -218.5$ ppm) with respect to that of Pd analogue **2** ($\delta = -182.6$ ppm), we became intrigued by the possibility of this difference being a HALA relativistic effect rather than a structural effect, which also provides new insight into the bonding situations of these complexes. The availability of the structurally very similar complexes **1**–**3** (Figure 1) with light and heavy metals allows a systematic analysis of the origin of metal-induced relativistic effects on ^{29}Si NMR properties. The Pt compound **1** in particular represents an ideal candidate for evaluating the computational model by considering three (sets of) parameters: isotropic NMR shift, chemical shift anisotropy (CSA) parameters, and $J_{Pt,Si}$ coupling. During the course of this study, we found that the presence of the heavy Pt atom close to Si has a particularly strong impact on the tensorial properties of the Si magnetic shielding. We aim to

[*] Dr. L. A. Truflandier, Prof. Dr. J. Autschbach
Department of Chemistry, 312 Natural Sciences Complex
State University of New York at Buffalo
Buffalo, NY 14260-3000 (USA)
Fax: (+1) 716-645-6963
E-mail: jochena@buffalo.edu
Dr. E. Brendler
Institut für Analytische Chemie
Technische Universität Bergakademie Freiberg
09596 Freiberg (Germany)
Dr. J. Wagler
Institut für Anorganische Chemie
Technische Universität Bergakademie Freiberg
09596 Freiberg (Germany)
E-mail: joerg.wagler@chemie.tu-freiberg.de

[**] This work has been supported by the National Science Foundation (CHE 0447321 and 092253).

Supporting information for this article is available on the WWW under http://dx.doi.org/10.1002/anie.201005431.

show herein that magic-angle spinning (MAS) NMR spectra recorded at a relatively low rotational frequency contain a clear signature of this relativistic effect.

For a systematic investigation, two new compounds were synthesized: a new solvate of Pt compound **1** (crystallized from *o*-dichlorobenzene, *o*-dcb) which comprises only one Si site in the crystallographic asymmetric unit (to obtain less complicated ^{29}Si CP/MAS NMR spectra), and the Ni compound **3** (Figures 1 and 2), which completes the triad. Their molecular structures were determined by X-ray crystallography.[11] For experimental procedures see the Supporting Information.

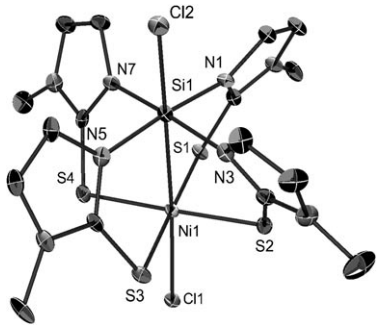

Figure 2. ORTEP representation of the predominant molecule of **3** in the crystal structure of its chloroform solvate (H atoms omitted; ellipsoids set at 30% probability).

The solid-state structure of **1**·(*o*-dcb) comprises molecule **1** situated on a crystallographic twofold axis. Apart from this feature, the molecular structure of **1** is similar to that of its chloroform solvate, which was reported earlier. Selected bond lengths [Å] of **1** in **1**·(*o*-dcb) are: Pt–Cl 2.629(2), Pt–S 2.328(1), 2.338(1), Pt–Si 2.457(2), Si–Cl 2.218(3), Si–N 1.903(4), 1.910(4). The crystal structure of Ni compound **3** (its chloroform solvate) is isostructural with the chloroform solvates of **1** and **2** and therefore comprises three independent Si sites in the ratio 1:1:4. Selected bond lengths [Å] of the predominant molecule of **3** (on Wyckoff position 8c in space group *P*4*nc*) are: Ni–Cl 2.612(1), Ni–S 2.228(1)–2.233(1), Ni–Si 2.598(1), Si–Cl 2.143(1), Si–N 1.871(3)–1.892(3). In sharp contrast with the metallasilatrane-like Ni complexes reported by Grobe et al.,[12] which exhibit Ni···Si separations of approximately 4 Å, compound **3** represents the first Si complex with a 3d TM as a lone-pair donor in a genuine TM→Si bonding situation. The experimental data (NMR shifts and atomic coordinates from XRD) obtained from the *o*-dcb solvate of **1** and the predominant sites in the chloroform solvates of **2** and **3** are considered below and denoted as Pt→Si, Pd→Si, and Ni→Si complexes, respectively.

For comparison of the relative influence of spin–orbit effects on the ^{29}Si NMR shifts along this triad, we performed scalar relativistic (SR) and spin–orbit (SO) relativistic computations. The data are collected in Table 1 and Figure 3. To probe the reliability of the theoretical method, a benchmark

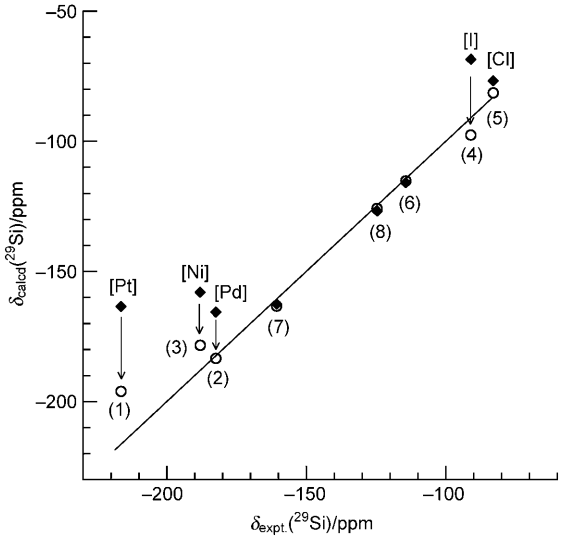

Figure 3. Correlation between experimental and theoretical ^{29}Si chemical shifts obtained for a benchmark set of silicon complexes **4**–**7** (see the Supporting Information) and the triad **1**–**3**. Diamonds: scalar ZORA, circles: spin–orbit ZORA. The solid line indicates perfect agreement between theoretical and experimental results.

for penta- and hexacoordinate silicon compounds presented in Figure S1 in the Supporting Information was performed. For molecules **6** and **7**, in which the silicon atom is surrounded by light nuclei, the agreement between theoretical and experimental results obtained for the SR and SO methods demonstrates the good accuracy of this approach. If systems with iodine (and even chlorine) bound to Si (molecules **4** and **5**) are considered, we observe NHD,[13–15] that is, stronger

Table 1: Calculated and experimental NMR parameters of the Pt-, Pd-, and Ni-containing complexes **1**, **2**, and **3**, respectively.

	δ_{iso} [ppm]		Ω [ppm][a]		κ[a]		K [10^{19} T^2 J^{-1}][b]		$\lvert ^1J(^{29}Si\text{-}^{195}Pt)\rvert$ coupling [Hz]
Complex	Scalar	Spin–orbit	Scalar	Spin–orbit	Scalar	Spin–orbit	PSO[c]	FC[c]	
Pt→Si	−163.5	−196.1	103.2	31.2	0.88	0.47	−45.2	2079.1	1047
Expt.		−216.4		27.5		−0.09			920
Pd→Si	−165.6	−183.4	84.9	56.1	0.92	0.86	−13.4	274.1	
Expt.		−182.4		46.5		0.17			–
Ni→Si	−158.0	−178.4	88.7	57.3	0.86	0.73	−13.6	51.5	
Expt.		−188.0		62.5		−0.06			–

[a] Definitions of the span (Ω) and the skew (κ) for the chemical shift are given in the Supporting Information. [b] Calculated reduced coupling constant at the SO-ZORA-PBE level of theory. The J coupling constant and K are related by $J_{A,B} = h/(4\pi^2)\gamma_A\gamma_B K_{A,B}$. [c] Paramagnetic and Fermi contact contributions. The diamagnetic and spin dipole are reported in Table S2 in the Supporting Information.

shielding induced by the halogen substituent at the SO level of theory, which then gives an excellent match with the experimental data. Such a phenomenon has also been discussed previously for silicon tetrahalides.[16]

The calculated chemical shifts obtained for the triad of Figure 1 are within 7.6 ppm of each other at the SR level, with deviations $\Delta\delta(^{29}\mathrm{Si})$ from the experimental results of 52.9, 30.0, and 16.8 ppm for Pt, Ni, and Pd, respectively. The same trend was obtained using a nonrelativistic approach. If the calculations include spin–orbit coupling, the agreement with experimental results improves nicely, with $\Delta\delta(^{29}\mathrm{Si}) = 20.3$, 9.6, and 1.0 ppm for Pt, Ni, and Pd, respectively (Figure 3). These residual deviations are within the expected error margins of the calculations arising from approximations in the density functional, the basis set, and other approximations in the computational model.

The SO calculation for the Pt complex yields a ^{29}Si chemical shift that is in substantially better agreement with experimental results, and signifies a HALA effect similar to the NHD known for heavy halide substitutions. However, in this case, the HALA effect is induced by a transition metal.

On the basis of structural XRD data of the initial report with M–Si distances of 2.46 and 2.57 Å for the Pt and Pd systems, respectively, it was argued that the chemical shift trends are related to the M–Si distances. However, the computations point to an electronic relativistic effect, that is, the variation of δ^{29}Si observed for **1**–**3** originates mainly from SO effects at the metal center. This result was confirmed by analysis of the different contributions of the computed shielding (see Table S1 in the Supporting Information), which indicates small variations of the paramagnetic term (below 4 ppm) along the metal triad while the spin–orbit component comprises between 30 and 40 ppm.

Closer inspection of Table 1 shows that the NHD-like influence on the isotropic ^{29}Si shift is not the only notable relativistic effect in the Pt system. An even stronger change, relatively speaking, is the reduction of the CSA tensor span (Ω) from 103.2 to 31.2 ppm upon inclusion of SO coupling in the calculations (to about $^1/_3$ of the SR value). Similar trends were also observed, but to a much lesser extent, for the Pd and Ni complexes (see Table 1). Motivated by this intriguing influence of relativity on the shielding tensor of a relatively light nucleus (Si), we simulated MAS spectra of the Pt system and acquired new experimental data at $\nu_{spin} = 700$ Hz to enhance the signature of κ and Ω in the spectrum. As depicted in Figure 4, the spectrum calculated with the spin–orbit data is in very good agreement with experimental results, whereas the SR spectrum has a completely different appearance. Strong $^1J_{Pt,Si}$ coupling leads to the observation of ^{195}Pt satellites on the experimental ^{29}Si spectra, allowing evaluation of the coupling constant to be around 920 Hz for **1**·(*o*-dcb). A calculation at the SO level yielded 1047 Hz (Table 1). The relative deviation from the experimental results is within the error margins of the theoretical method,[17] and the agreement with experimental results overall is very satisfactory. The decomposition of the coupling constant for this and the other two systems showed that the Fermi contact mechanism is the dominant contribution.

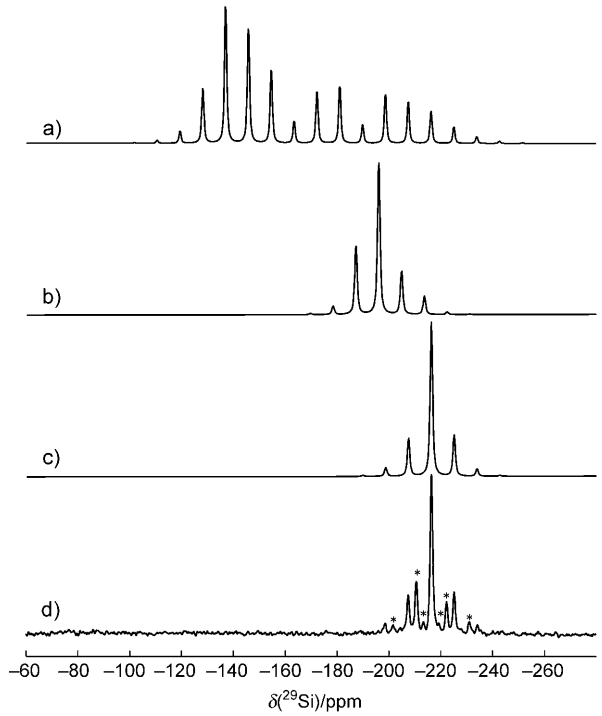

Figure 4. Experimental and theoretical ^{29}Si CP/MAS NMR spectra of the Pt→Si complex **1**·(*o*-dcb) obtained at $B_0 = 9.4$ T, $\nu_{spin} = 700$ Hz. a) Scalar ZORA, b) spin–orbit ZORA, c) simulated from the experimental NMR parameters, and d) experimental CP/MAS spectrum. Stars indicate the ^{195}Pt satellites associated with the isotropic signal and the spinning side bands.

The $J_{Pt,Si}$ coupling in **1** hints at notable covalent contributions to the Pt–Si bonding, thus raising the question as to the applicability of the "metallasilatrane" (metalla to sila site trans annular dative bond) model Pt→Si. Analysis of the bonding in compounds **1**–**3** revealed very interesting electronic structures, which strongly depend on the Group 10 metal. A natural bond orbital (NBO) analysis using a bond occupation threshold of 1.7 indicated a significant amount of delocalized electronic charge (above 7 *e*) in the triad, partially in the heterocyclic ligands but also in the S_4M–Si moieties. Within the triad, the M→Si bond in the Pt system is the most covalent (Table S3 in the Supporting Information) and has the highest s character on both the M and Si atom, a prerequisite for large Fermi contact *J* couplings. The Si s character helps to rationalize the particularly strong SO effect on its shielding tensor. We recall that SO-induced HALA effects have an electronic mechanism related to the spin mechanisms of *J* coupling[2,15,18] and are particularly effective when there are strong covalent bonds with significant s character connecting the heavy and the light atom.

The calculated electronic relaxation energies ΔE_{relax} with respect to promolecular fragments (Table S3 in the Supporting Information) indicate that the strength of the interaction of a M^{2+} center with the fragments $Cl[Si(\mu\text{-mt})_4]^-$ (mt = 2-mercapto-1-methylimidazolide) and Cl^- is enhanced by 60 kcal mol^{-1} for the Pt system, whereas the values are virtually identical for Ni→Si and Pd→Si. The main source for this difference is the orbital relaxation term ΔE_{orb}, which

corroborates the results from the NBO analysis. The Wiberg bond indices listed in Table S3 also point to Pt→Si as the most covalent system, although with the large basis sets used for Pt and Si, this criterion might not be particularly reliable. The NBO analysis showed that the M→Si bonds are mainly formed through donation of charge from the d_{z^2} lone pairs of the metal atoms to Si. Thus, the notation $XL_4M{\rightarrow}SiL_4'X$ is more appropriate than $XL_4M{-}SiL_4'X$, as supported by the localization of the bond orbital on the metal center (see Figure S3 in the Supporting Information), in particular for Ni and Pd. The reorganization of charge relative to promolecular fragments is also shown in form of deformation density plots in Figure 1. A stronger accumulation of electron density between Pt and Si compared with the Ni and Pd systems is yet another indicator of the stronger covalency in this system. We also note the deformation density in the S_4 plane and around the M-bound Cl atom. These findings are reinforced by an analysis of the electron-localization functions (Figures S2 and S3).

Table 1 and Figure 3 reveal that there is also a sizable SO effect on the Si shielding tensor in the Ni and Pd compounds. Relativistic effects scale formally as Z^2 with the charge Z of a heavy nucleus and are not negligible for S (compare also the SO effect from Cl on system **5**, Figure S1 and Table S1) or Si itself. In complexes **1**–**3**, some of the SO contributions may be attributed to the sulfur atoms because of the strong electron delocalization in the cores of the complexes, which thus help to rationalize the unexpectedly large SO effect in the Ni→Si complex **3**. Hyvärinen et al. recently reported uncharacteristically large SO effects on proton shifts in Co^{III} polyamine complexes relative to Rh and Ir analogues, in part related to the larger ligand-field splitting for the heavier metals,[15b] a trend that we also found for **1**–**3**. For additional discussion of the Ni system, refer to the Supporting Information.

In conclusion, we have presented the first crystallographically and ^{29}Si NMR spectroscopically characterized compound with a 3d TM→Si dative bond. NBO and electron density analyses of three related paddlewheel-shaped complexes [ClTM(μ-mt)$_4$SiCl] of the metal triad confirmed the applicability of a TM→Si dative bonding model, especially for TM = Ni and Pd, whereas the Pt analogue exhibits notable covalent contributions. For these compounds, the ^{29}Si NMR spectroscopic properties (isotropic shift, features of the CSA tensor, and $J_{Pt,Si}$ coupling constant) were successfully modeled by taking relativistic effects, including spin–orbit (SO) coupling, into account. SO effects on the ^{29}Si NMR properties were also proven for the Pd→Si and even the Ni→Si system. The latter demonstrates that considering these kinds of relativistic effects adds to an understanding of electronic features of heavy atom–lighter atom bonding, even if the heavy atom is a comparatively light TM atom. The lighter atom bonding partner and other ligands (such as S and Cl atoms) may also contribute to the magnitude of the overall SO effects in the NMR spectrum. In both the investigation of classical transition-metal complexes (e.g., Ni complexes with alumylene, silylene, or silyl ligands,[19] for purposes such as catalyst applications) and the elucidation of novel bonding situations (e.g., in compounds such as metallaboratranes[20]), models aware of spin–orbit coupling effects may therefore prove to be valuable tools for the analysis of NMR spectra, even in the absence of truly heavy elements. For example, spin–orbit NMR effects appear to be a sensitive probe for the extent of electron sharing or delocalization between a given nucleus and heavy atoms in its surrounding ligand sphere.

Experimental Section

Density functional theory computations were performed with the Amsterdam density functional (ADF)[21] package using experimental geometries (from XRD data), employing the relativistic zeroth-order regular approximation (ZORA)[22] Hamiltonian for the ground state and for the shielding tensor[23] and *J* coupling[24–26] calculations, and the VWN + PBE functionals[27–29] along with triple-zeta Slater-type basis sets with multiple sets of polarization functions. For complete details, see the Supporting Information.

Synthesis of compound **3**: In a Schlenk tube, tris(methimazolyl)-chlorosilane[10] (1.72 g, 4.27 mmol) and $[NiCl_2(PPh_3)_2]$ (1.40 g, 2.14 mmol) were layered with chloroform (15 mL) and stored at room temperature for 1 week, whereupon the solid product was separated from the supernatant by decantation, washed with chloroform (2 × 2 mL), and briefly dried in vacuo. Yield: 0.66 g (0.71 mmol, 33 %). C,H,N,S microanalysis: found (%): C 23.03, H 2.50, N 11.99, 13.17; calcd for $C_{56}H_{68}Cl_{30}N_{24}Ni_3S_{12}Si_3$: C 24.14, H 2.46, N 12.07, S 13.81. (Chloroform content that exceeds the composition $(\mathbf{3})_3$-$(CHCl_3)_8$ might be responsible for the slightly lower C,N,S content.)

Received: August 30, 2010
Published online: November 29, 2010

Keywords: heterometallic complexes · nickel · NMR spectroscopy · relativistic effects · silicon

[1] P. Pyykkö, *Chem. Rev.* **1988**, *88*, 563 – 594.
[2] J. Autschbach, S. Zheng, *Annu. Rep. NMR Spectrosc.* **2009**, *67*, 1 – 95.
[3] M. A. M. Forgeron, R. E. Wasylishen, G. H. Penner, *J. Phys. Chem. A* **2004**, *108*, 4751 – 4758.
[4] A. M. Kantola, P. Lantto, J. Vaara, J. Jokisaari, *Phys. Chem. Chem. Phys.* **2010**, *12*, 2679 – 2692.
[5] A. Bagno, R. Bini, *Angew. Chem.* **2010**, *122*, 1101 – 1104; *Angew. Chem. Int. Ed.* **2010**, *49*, 1083 – 1086.
[6] J. Autschbach, A. M. Kantola, J. Jokisaari, *J. Phys. Chem. A* **2007**, *111*, 5343 – 5348.
[7] J. Macháček, J. Plešek, J. Holub, D. Hnyk, V. Všetečka, I. Císařová, M. Kaupp, B. Štíbr, *Dalton Trans.* **2006**, 1024 – 1029.
[8] a) F. Chen, G. Ma, G. M. Bernard, R. G. Cavell, R. McDonald, M. J. Ferguson, R. E. Wasylishen, *J. Am. Chem. Soc.* **2010**, *132*, 5479 – 5493; b) D. L. Bryce, N. M. D. Courchesne, F. A. Perras, *Solid State Nucl. Magn. Reson.* **2009**, *36*, 182 – 191; c) K. W. Feindel, R. E. Wasylishen, *Can. J. Chem.* **2004**, *82*, 27 – 44.
[9] P. Gualco, T.-P. Lin, M. Sircoglou, M. Mercy, S. Ladeira, G. Bouhadir, L. M. Pérez, A. Amgoune, L. Maron, F. P. Gabbaï, D. Bourissou, *Angew. Chem.* **2009**, *121*, 10076 – 10079; *Angew. Chem. Int. Ed.* **2009**, *48*, 9892 – 9895.
[10] J. Wagler, E. Brendler, *Angew. Chem.* **2010**, *122*, 634 – 637; *Angew. Chem. Int. Ed.* **2010**, *49*, 624 – 627.
[11] CCDC 782201 (**1**·(*o*-dcb)) and 782200 ($(\mathbf{3})_3(CHCl_3)_8$) contain the supplementary crystallographic data for this paper. These data can be obtained free of charge from The Cambridge Crystallographic Data Centre via www.ccdc.cam.ac.uk/data_request/cif. Space group, cell parameters, and *R* values with $[I > 2\sigma(I)]$: **1**·(*o*-dcb): *C*2/*c*, *a* = 14.6661(5), *b* = 13.0656(5), *c* = 16.3558(6) Å, *β* =

108.494(2)°, $R_1 = 0.0352$, $wR_2 = 0.0548$; $(\mathbf{3})_3(CHCl_3)_8$: *P*4*nc*, $a = 19.0811(1)$, $c = 27.8423(3)$ Å, $R_1 = 0.0390$, $wR_2 = 0.0898$.

[12] a) J. Grobe, R. Wehmschulte, B. Krebs, M. Läge, *Z. Anorg. Allg. Chem.* **1995**, *621*, 583 – 596; b) J. Grobe, N. Krummen, R. Wehmschulte, B. Krebs, M. Läge, *Z. Anorg. Allg. Chem.* **1994**, *620*, 1645 – 1658.

[13] R. G. Kidd, *Annu. Rep. NMR Spectrosc.* **1980**, *10*, 1 – 79.

[14] R. G. Kidd, *Annu. Rep. NMR Spectrosc.* **1991**, *23*, 85 – 139.

[15] a) M. Kaupp, O. L. Malkina, V. G. Malkin, P. Pyykkö, *Chem. Eur. J.* **1998**, *4*, 118 – 126; b) M. Hyvärinen, J. Vaara, A. Goldammer, B. Kutzky, K. Hegetschweiler, M. Kaupp, M. Straka, *J. Am. Chem. Soc.* **2009**, *131*, 11909 – 11918.

[16] H. Nakatsuji, T. Nakajima, M. Hada, H. Takashima, S. Tanaka, *Chem. Phys. Lett.* **1995**, *247*, 418 – 424.

[17] S. Moncho, J. Autschbach, *J. Chem. Theory Comput.* **2010**, *6*, 223 – 234.

[18] Y. Nomura, Y. Takeuchi, N. Nakagawa, *Tetrahedron Lett.* **1969**, *10*, 639 – 642.

[19] a) A. Meltzer, C. Präsang, C. Milsmann, M. Driess, *Angew. Chem.* **2009**, *121*, 3216 – 3219; *Angew. Chem. Int. Ed.* **2009**, *48*, 3170 – 3173; b) M. T. Whited, N. P. Mankad, Y. Lee, P. F. Oblad, J. C. Peters, *Inorg. Chem.* **2009**, *48*, 2507 – 2517; c) T. Steinke, C. Gemel, M. Cokoja, M. Winter, R. A. Fischer, *Angew. Chem.* **2004**, *116*, 2349 – 2352; *Angew. Chem. Int. Ed.* **2004**, *43*, 2299 – 2302; d) W. Chen, S. Shimada, M. Tanaka, Y. Kobayashi, K. Saigo, *J. Am. Chem. Soc.* **2004**, *126*, 8072 – 8073; e) S. Shimada, M. L. N. Rao, T. Hayashi, M. Tanaka, *Angew. Chem.* **2001**, *113*, 219 – 222; *Angew. Chem. Int. Ed.* **2001**, *40*, 213 – 216.

[20] a) M. Sircoglou, S. Bontemps, G. Bouhadir, N. Saffon, K. Miqueu, W. Gu, M. Mercy, C.-H. Chen, B. M. Foxman, L. Maron, O. V. Ozerov, D. Bourissou, *J. Am. Chem. Soc.* **2008**, *130*, 16729 – 16738; b) J. S. Figueroa, J. G. Melnick, G. Parkin, *Inorg. Chem.* **2006**, *45*, 7056 – 7058; c) A. F. Hill, G. R. Owen, A. J. P. White, D. J. Williams, *Angew. Chem.* **1999**, *111*, 2920 – 2923; *Angew. Chem. Int. Ed.* **1999**, *38*, 2759 – 2761.

[21] E. J. Baerends et al., ADF 2009, SCM; Theoretical Chemistry, Vrije Universiteit, Amsterdam.

[22] E. van Lenthe, E. J. Baerends, J. G. Snijders, *J. Chem. Phys.* **1993**, *99*, 4597 – 4610.

[23] S. K. Wolff, T. Ziegler, E. van Lenthe, E. J. Baerends, *J. Chem. Phys.* **1999**, *110*, 7689 – 7698.

[24] J. Autschbach, T. Ziegler, *J. Chem. Phys.* **2000**, *113*, 9410 – 9418.

[25] J. Autschbach, T. Ziegler, *J. Chem. Phys.* **2000**, *113*, 936 – 947.

[26] J. Autschbach, *ChemPhysChem* **2009**, *10*, 2274 – 2283.

[27] S. H. Vosko, L. Wilk, M. Nusair, *Can. J. Phys.* **1980**, *58*, 1200 – 1211.

[28] J. P. Perdew, K. Burke, M. Ernzerhof, *Phys. Rev. Lett.* **1996**, *77*, 3865 – 3868.

[29] B. Hammer, L. B. Hansen, J. K. Nørskov, *Phys. Rev. B* **1999**, *59*, 7413 – 7421.

